Per. Mineral. (1999), *68*, 3, 275-286

PERIODICO di MINERALOGIA
established in 1930

An International Journal of
MINERALOGY, CRYSTALLOGRAPHY, GEOCHEMISTRY, ORE DEPOSITS, PETROLOGY, VOLCANOLOGY
and applied topics on *Environment, Archaeometry* and *Cultural Heritage*

Phase relationships in hydrous peridotites at high presssure: preliminary results of multianvil experiments

PATRIZIA FUMAGALLI* and STEFANO POLI

Dipartimento di Scienze della Terra, Università degli Studi di Milano, Via Botticelli 23, I-20133 Milano, Italy

Submitted, July 1999 - Accepted, November 1999

ABSTRACT. — Phase relationships in hydrous peridotite at high pressure are investigated running experiments in a multianvil apparatus at 4.6-5.2 GPa pressures, 680-750°C temperatures and fluid saturated conditions in the peridotite model system Na_2O-CaO-FeO-MgO-Al_2O_3-SiO_2-H_2O (NCFMASH). Pressure calibration was carried out both at room temperature using the transitions Bi I-II and Bi III-V (occurring at 2.55 GPa and 7.7 GPa, respectively), and at 1000°C using the phase transitions coesite-stishovite and garnet-perovskite structure in Ca-germanates (occurring at 8.7 and 6.1 GPa, respectively). Run durations were from 110 to 170 hours. Run products were identified by X-ray powder diffraction, back-scattered and secondary electron images and microprobe analysis.

In an Al-enriched peridotite, the assemblage olivine, clinopyroxene, garnet, 10Å phase was found at 5.2 GPa 680°C. Since the crystal structure of the 10Å phase is broadly similar to micas, this phase can incorporate more than 0.8 atoms per formula unit (a.p.f.u.) of aluminium. However diffraction patterns do not exclude the occurrence of hydrous mixed-layered structures at these conditions. Although in the simple system MgO-SiO_2-H_2O the assemblage 10Å phase + forsterite is incompatible with the join enstatite + H_2O, all these phases may coexist in Fe- and Al-bearing systems (lherzolites and pyroxenites). At 4.6 GPa 750°C the anhydrous assemblage olivine, clinopyroxene, orthopyroxene, garnet is stable. Phase abundances obtained by Rietveld refinement are in agreement with those obtained by mass balance and present evidence for the reaction 10Å phase = enstatite + pyrope + H_2O.

The occurrence of the 10Å phase at pressures above the chlorite stability field promotes H_2O transfer to Dense Hydrous Magnesium Silicates (DHMS) and H_2O transport into the deep mantle (> 200km depth).

RIASSUNTO. — In questo studio sono state investigate le relazioni di fase in peridotiti idrate ad alta pressione. A tale scopo sono stati eseguiti esperimenti con l'apparato multianvil nel sistema modello Na_2O-CaO-FeO-MgO-Al_2O_3-SiO_2-H_2O (NCFMASH) a pressioni comprese tra 4,6 e 5,2 GPa e temperature tra 680 e 750°C in condizioni di saturazione di fluido. La calibrazione della pressione è stata effettuata sia a temperatura ambiente, utilizzando le transizioni di fase del Bismuto (Bi I-II a 2,55 GPa e Bi III-V a 7,7 GPa), sia a 1000 °C mediante la transizione coesite-stishovite a 8,7 GPa e la trasformazione da struttura granato a struttura perovskite nei germanati di calcio a 6,1 GPa. Gli esperimenti hanno avuto durate comprese tra 110 e 170 ore. I prodotti ottenuti sono stati caratterizzati mediante diffrazione a raggi X su polveri, immagini di elettroni retrodiffusi e secondari e microsonda elettronica.

* Corresponding author, E-mail: patrizia@expe.terra.unimi.it

A 5,2 GPa e 680°C è stata riconosciuta l'associazione olivina-clinopirosseno-granato-fase 10Å. Come risultato di una struttura simile a quella delle miche, la fase 10Å può incorporare fino a 0,8 atomi per formula unitaria di alluminio. Ciò nonostante il profilo di diffrazione non permette di escludere la presenza di strutture a strati misti stabili a tali condizioni. Tuttavia, sebbene l'associazione fase 10Å + forsterite sia incompatibile con la *tie-line* enstatite + H_2O nel sistema modello MgO-SiO_2-H_2O, la presenza di tutte queste fasi è possibile in sistemi più complessi contenenti Fe e Al (lherzoliti e pirosseniti). A 4,7 GPa e 750°C è stata riconosciuta l'associazione anidra olivina-clinopirosseno-ortopirosseno-granato. L'abbondanza delle fasi ottenuta mediante il metodo Rietveld è in accordo con il bilancio di massa e permette di riconoscere la reazione: fase 10Å = enstatite + piropo + H_2O.

La presenza della fase 10Å a pressioni superiori al campo di stabilità della clorite promuove il trasferimento di H_2O a fasi appartenenti al gruppo dei silicati magnesiaci ad alta densità (Dense Hydrous Magnesium Silicates, DHMS) e quindi il trasporto di H_2O nel mantello a profondità superiori a 200 km.

KEY WORDS: *high pressure experiments, multi-anvil, hydrous peridotites, 10Å phase, subduction zones.*

INTRODUCTION

Hydrous phases are responsible for most of the petrological processes occurring at subduction zones where water is recycled into the mantle via dehydration reactions. Although ultramafic rocks may constitute 80% of the tota! slab volume, their relevance as water carriers in the deep levels of subduction zones largely depends on the degree of hydration they have undergone. In peridotites water is incorporated during hydrothermal exchange with sea water on the ocean floor. The occurrence of extensively serpentinized peridotites in a variety of tectonic settings, i.e. fast and slow spreading ridges (Frueh-Green *et al.*, 1995; Muller *et al.*, 1997), passive continental margins (Boillot *et al.*, 1998) and the stability of serpentine and associated hydrous phases at high and very high pressures in orogenic belts (Scambelluri *et al.*, 1995), suggests that the understanding of phase relationships involving hydrous phases in ultramafic systems at high pressure is fundamental to depict the evolution of subduction zones. Furthermore, due to the presence of volcanic arcs above subduction zones and the peculiar enrichment of island arc basalts in slab-derived components (e.g. ^{10}Be, Cl etc.), it is largely accepted that fluids released from the subducting lithosphere migrate into the overlying wedge, thereby affecting its composition, mineralogy and phase relations. Hydrous peridotites have been extensively modelled in the MgO-SiO_2-H_2O (MSH) and MgO-Al_2O_3-SiO_2-H_2O (MASH) chemical systems, where antigorite and chlorite are the major hydrous phases stable up to 150-200 km (Mysen *et al.*, 1998 and references therein). Based on experimental phase relations, it is presently accepted that, above the stability field of antigorite-chlorite assemblages, water is transferred to Dense Hydrous Magnesium Silicates (DHMS) such as 10Å phase and phase A (Ulmer and Trommsdorf, 1995). With the exception of a few natural occurrences as inclusions in olivine from peridotite-xenoliths (Khisina and Wirth, 1998; Wirth and Khisina, 1998), DHMS have been only synthesized in the model system MSH at pressures ranging from 3 to 20 GPa. The 10Å phase, first synthesized by Sclar *et al.* (1965), corresponds to a phyllosilicate chemically analogue to talc but with excess water (>5 wt% H_2O). The 10Å phase is identified on the basis of X-ray powder diffraction pattern by its basal peak at 2θ = 10Å, even though large broadening of the d-space value has been reported (Yamamoto and Akimoto, 1977). It forms by hydration of talc at pressure of 3-6 GPa and its upper thermal stability is 725°C at 6.0 GPa (Yamamoto and Akimoto, 1977; Pawley and Wood, 1995). The 10Å phase also occurs in association with olivine+H_2O as a breakdown product of serpentine (Ulmer and Trommsdorf, 1998). No upper pressure constraints on the 10Å phase stability are available yet. Despite considerable efforts made to sinthesize the 10Å phase in the simple system MSH, its relevance in more complex systems is still unexplored. The goal

of this work is to investigate the stability of 10Å phase and chlorite in the model peridotite system Na_2O-CaO-FeO-MgO-Al_2O_3-SiO_2-H_2O (NCFMASH) at P-T conditions above the stability of antigorite-bearing assemblages.

EXPERIMENTAL TECHNIQUES

Apparatus

High pressure experiments were carried out in a Walker-type multianvil apparatus at the Dipartimento di Scienze della Terra of Milano (for further details see Walker *et al.*, 1990). The multianvil module is mounted on a 1000-ton uniaxial press, driven by a hydraulic system of domestic design. A hydraulic pressure of 700 bars applied to the jack corresponds to an axial force of 1000 tons. Pressure is regulated by an electronically controlled screw worm jack. Tungsten carbide cubic anvils of 32 mm of edge and with 8 mm, 11 mm and 17 mm Truncation Edge Length (TEL) are available. Pressure cells are made of prefabricated MgO octahedra (containing 5 wt% Cr_2O_3) with 14 mm (14M), 18 mm (18M) and 25 mm (25M) edge length which are used with cubes of 8 mm, 11 mm and 17 mm of TEL, respectively. Preformed pyrophyllite gaskets are used as support for the pressure media. Stepped graphite furnaces are used in order to minimize the thermal gradient along the assembly and to localize the hot spot in the middle of the furnace (Walter *et al.*, 1995). 25M assembly furnaces (fig. 1) were prepared with a 18 mm long graphite cylinder (6 mm o.d., 5.2 mm i.d.) and a 4.5 mm long graphite cylinder (5.2 mm o.d., 4.2 mm i.d.) and placing the latter in the middle of the former. Noble metal capsules containing the starting material are placed in the hot spot of the furnace. An axial Pt-$Pt_{87}Rh_{13}$ thermocouple (type S) is in direct contact with the capsule. MgO spacers and ceramic insulators are placed around the capsule and the thermocouple. Graphite discs on both the ends of the assembly garantee electrical contact with the WC cubes.

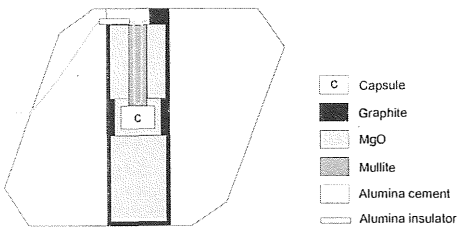

Fig. 1 – Assembly for multianvil experiments, octahedron with an edge length of 25 mm (25M), truncation edge length 17 mm (17TEL).

Pressure calibration

In order to determine the actual sample pressure as a function of the press-load, pressure calibration was performed both at room temperature, using the Bi I-II and Bi III-V phase transitions occurring at 2.6 and 7.7 GPa respectively (Lloyd, 1971), and at 1000°C by the transitions coesite-stishovite and garnet-perovskite structures in $CaGeO_3$ occurring at 8.7 GPa (Zhang *et al.* 1996) and 7.7 GPa (Susaki *et al.* 1985), respectively. Pressure calibration was performed for 14M, 18M and 25M pressure media. A bismuth foil 0.025 mm thick was used as starting material for the room temperature pressure calibration. Bismuth was placed in the middle of MgO cylinders. The electrical contact was provided by placing copper on both the ends of the assembly. The Bi I-II and Bi III-V phase transitions were identified measuring in-situ the drop of bismuth resistance. Using a 14M pressure cell the two transitions occur at oil pressure of 55.8 bars and 160 bars respectively. For the 18M at 102 bars and at 242 bars (fig. 2). Since the efficience of pressure generation is proportional to the size of the pressure cell, using a 25M octahedron it is not possible to observe the Bi III-V transition and only the Bi I-II transition was observed at 170 bars. Pressure calibration at high temperature (1000 °C) was carried out using as starting materials ground quartz powder plus coesite and stishovite and $CaGeO_3$ with wollastonite structure loaded in either Ag-Pd or Pt capsules (outer diameter of 2.4 mm and 1.7 mm

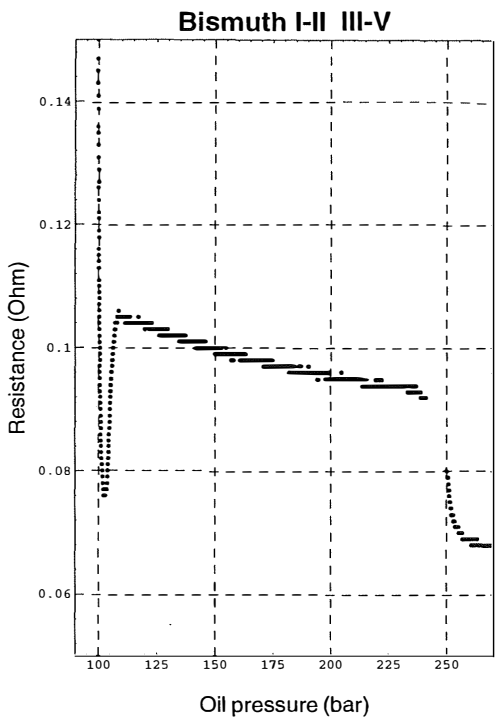

Fig. 2 – Pressure calibration at room temperature for the 18M. Two drops of the bismuth resistance have been measured in situ.

respectively). Reversal experiments were also performed using as starting material previous runs containing both reactants and products. Quenched products were identified by X-ray powder diffraction (XRD). Relevant experimental results of pressure calibration at high temperature are summarized in Table 1. Due to the short duration of the experiment GE1, the occurrence of garnet structure as run product was considered to be metastable. The occurrence of perovskite structure as unique phase in the longer run GE2 carried out at lower pressure further supports the above interpretation. Phase abundances, when available, have been evaluated by Rietveld refinement on X-ray powder diffraction profiles using the GSAS software (Larson and Von Dreele, 1998). Calibrations curves obtained for 14M, 18M and 25M pressure media are shown in fig. 3.

Starting materials and experimental procedures

The model peridotite system Na_2O-CaO-FeO-MgO-Al_2O_3-SiO_2-H_2O (NCFMASH) was investigated using seeded gels as starting material. Gels were prepared following the

TABLE 1

Run table of relevant calibration experiments. St: stishovite, Coe: coesite, Qtz: quartz, Pvs: perovskite structure in $CaGeO_3$, Gar: garnet structure in $CaGeO_3$.

Run	Cell pressure	T (°C)	Oil Pressure (bar)	Run duration	Run products
ST4	25M	1000	590	30’	St
ST12	25M	1000	500	27 h	St
ST13	25M	1000	430	2 h	Coe
ST14	25M	1000	465	6.5 h	St
GEl	25M	1000	370	15’	$CaGeO_3$ Pvs-Gar
GE2	25M	1000	360	60’	$CaGeO_3$ Pvs
GE3	25M	1000	300	52 h	$CaGeO_3$ Gar
ST3	18M	1000	270	15’	Coe
ST2	18M	950	290	5’	St-Qtz
ST7	14M	1000	180	20’	St (88%)-Coe (12%)
ST11	14M	800	170	5’	St

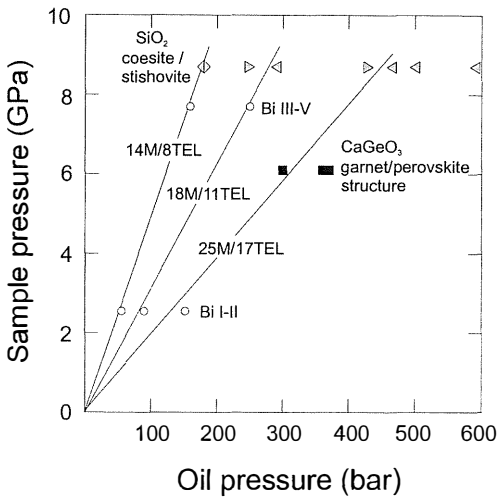

Fig. 3 – Calibration curves obtained for 14M, 18M and 25M pressure media. Triangles refer to coesite-stishovite transition, squares to garnet-perovskite structure in $CaGeO_3$ and circles to transformations in Bismuth.

method of Hamilton and Henderson (1968) using tetraethylorthosilicate (TEOS) as silica source, pure Na-, Ca-, Mg- and Al- nitric solutions, ferric benzoate and ammonium hydroxide. A mixture of seeds constituted of natural clinochlore (34.58 wt% in the seed mixture), natural pyrope (7.44 wt%), synthetic diopside (36.94 wt%) and synthetic forsterite (Fo_{80}, 21.04 wt%) were added to the gel in the proportion of 1:10. The bulk composition of the gel, peridotite D of Mysen and Boettcher (1975), is shown in Table 2. This extremely Al- and Ca-enriched starting material has been chosen in order to maximize the occurrence of aluminous phases. A similar approach has been used by Niida and Green (1999) to investigate the crystal chemistry of amphibole in ultramafic rocks. As an example, the composition of starting material HPY-40% OL of Niida and Green (1999) closely approach the composition of Gel D used in this study. Gold capsules (outer diameter of 3.0 mm, length of 3.5-4.5 mm) were welded after being loaded with 10-15 mg of seeded gel and 10 wt% of distilled water. All runs were at fluid saturated conditions. Experiments were performed at pressures ranging from 4.6 to 5.2 GPa and temperatures from 680 to 750°C. Oxygen fugacity was buffered by adding graphite into the capsule. As experimental temperatures were relatively low, runs lasted up to 170 hours. Pressure uncertainties, largely depending on the accuracy of the calibrant reaction, were assumed to be ± 4%. Temperature was considered accurate to ± 20 °C without taking into account the effect of pressure on the e.m.f. of the thermocouple.

Quenched run products were first characterized by conventional X-ray powder diffraction on a Philips PW1000 diffractometer and carefully inspected by back-scattered and secondary electron images. An ARLK microprobe with six spectrometers was used for electron probe microanalyses. Beam conditions were 15 kV and 20 nA. Silicates were used as standards and data processed with a standard ZAF correction procedure. Quantitative evaluation of phase abundances were obtained both by Rietveld refinement on X-ray powder diffraction profiles and mass balance calculations.

Results

Experimental results are shown in Table 3. Run products obtained at 5.2 GPa and 680°C (Chl3) and at 4.8 GPa and 680°C (Chl5) consist of garnet, olivine, clinopyroxene and a

TABLE 2

Bulk composition of starting material which corresponds to peridotite D of Mysen and Boettcher (1975). Total iron as Fe_2O_3.

Oxide	**Gel D (wt%)**
SiO_2	44.82
Al_2O_3	8.21
Fe_2O_3	10.86
MgO	26.53
CaO	8.12
Na_2O	0.89
Total	99.43
X_{Mg}	0.83

TABLE 3

Experimental results obtained in the system Na_2O-CaO-FeO-MgO-Al_2O_3-SiO_2-H_2O. gar: garnet; cpx:clinopyroxene; ol:olivine; opx:orthopyroxene; 10Å: 10Å phase.

Run	Pressure (GPa)	Temperature (°C)	Run duration (h.)	Starting material	Run products
Chl2	4.6	750	111	Gel D	gar, cpx, ol, opx
Chl3	5.2	680	170.4	Gel D	10Å, gar, cpx, ol
Chl5	4.8	680	151.3	Gel D	10Å, gar, cpx, ol

hydrous phase. The latter was identified as the 10Å phase on the basis of X-ray powder diffraction due to the basal peak at 8.6 degrees of two theta (d = 10.3Å). The 10Å phase forms aggregates (10-15 μm) of platy crystals observed both in back-scattered and secondary electron images (fig. 4). BSE images show well crystallized garnets (up to 10 μm) in a finer matrix constituted of olivine and clinopyroxene intergrowths. Garnet and olivine seeds are often preserved as core of new formed crystals. At 5.2 GPa and 750°C (Chl2) the anhydrous assemblage garnet, olivine, clinopyroxene and orthopyroxene was found to be stable. Texturally Chl2 is similar to runs Chl3 and Chl5 although garnet is more abundant and the finer matrix contains in addition orthopyroxene.

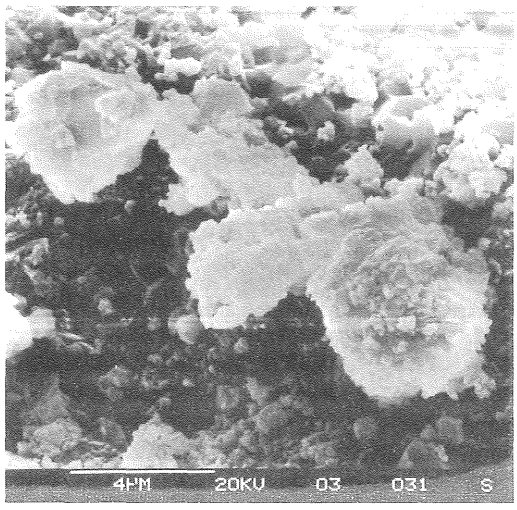

Fig. 4 – SEM image of aggregates of platy crystals of 10Å phase obtained at 4.8 GPa and 650°C.

Mineral compositions are summarized in Table 4. Compared to rock-forming minerals of natural garnet lherzolites of Cima di Gagnone (Evans and Trommsdorf, 1978) and Nonsberg (Obata and Morten, 1987), the compositions of synthesized phases display lower X_{Mg} ($Mg/(Fe^{2+}+Mg)$), which is in agreement with the lower bulk X_{Mg} of the starting material (X_{Mg}=0.83 against X_{Mg}=0.90-0.95 of Cima di Gagnone and Nonsberg lherzolites). Clinopyroxenes show enstatite+ferrosilite contents ranging from 13 to 19%, i.e. a value much higher than the ones measured in natural clinopyroxenes where this component ranges from 2% (Cima di Gagnone) to 5% (Nonsberg). Although data are absent for the solvus orthopyroxene-clinopyroxene for ultramafic compositions when sodium is a relatively abundant component, the effect of sodium may be envisaged as responsable for the larger extent of solution between orthopyroxene and clinopyroxene. The 18% of jadeitic component in clinopyroxene is high compared to natural clinopyroxenes, which range from 2% (Cima di Gagnone) to 6.7% (Nonsberg). Since clinopyroxene is the only sodium bearing phase, this higher jadeitic component reflects the high Na content of the bulk composition (0.89 wt%). Microanalyses on aggregates of the 10Å phase show that it incorporates up to 0.8 atoms p.f.u. of aluminium. 10Å phase is a phyllosilicate chemically analogue to talc but

TABLE 4

Mineral chemistry. Opx: orthopyroxene, 10Å: 10Å phase. Chl2: 4.6 GPa-750°C; Chl3: 5.2 GPa-680°C.

	Olivine		**Clinopyroxene**		**Garnet**		**Opx**	**10Å**
	Chl2	*Chl3*	*Chl2*	*Chl3*	*Chl2*	*Chl3*	*Chl2*	*Chl3*
SiO_2	41.17	40.98	53.01	54.84	41.94	41.73	57.13	44.93
Al_2O_3	0.02	0.13	2.94	4.00	22.33	22.05	0.30	10.72
Fe_2O_3	0.00	0.00	0.00	0.00	0.38	0.00	2.06	0.00
FeO	13.31	12.73	5.03	4.70	15.63	18.93	6.46	4.56
MgO	46.00	45.20	19.37	14.96	14.64	12.84	34.38	28.14
CaO	0.06	0.22	18.34	17.94	6.26	5.87	0.24	0.34
Na_2O	0.00	0.00	1.26	2.39	0.09	0.01	0.00	0.00
Total	100.56	99.26	99.95	98.83	101.27	101.44	100.57	88.80
Si	1.021	1.029	1.925	2.000	3.041	3.062	1.968	2.900
Al	0.001	0.004	0.126	0.172	1.909	1.907	0.012	0.816
Fe^{3+}	0.000	0.000	0.000	0.000	0.021	0.000	0.053	0.000
Fe^{2+}	0.276	0.267	0.153	0.143	0.948	1.162	0.187	0.246
Mg	1.701	1.692	1.049	0.813	1.582	1.404	1.769	2.708
Ca	0.002	0.006	0.713	0.701	0.487	0.462	0.009	0.235
Na	0.000	0.000	0.089	0.169	0.012	0.001	0.000	0.000
X_{Mg}	0.859	0.859	0.873	0.850	0.522	0.463	0.881	-
X_{Ca}	-	-		-	0.161	0.152		

with excess water. Its structure has been related to that of 2:1 trioctahedral phyllosilicate structure such as phlogopite (Bauer and Sclar, 1981). On the basis of IR spectroscopy and thermal analysis Bauer and Sclar (1981) indicated that water molecules occupy the interlayer 12-coordinated sites of a mica-like structure and interact with hydroxyl groups of the octahedral layers. This leads to the formation of oxonium ions and oxygens ions and to the new structural-chemical formula $H_3O^+ \cdot Mg_3Si_4O_{10}(OH)$. However, the 10Å phase is strictly not a member of mica family and does not form solid solution with K-bearing series (Bauer and Sclar, 1981). Nevertheless, as a result of structural similarity to micas and talc, it is therefore likely that some aluminium is incorporated in the 10Å phase.

DISCUSSION

Full-profile Rietveld refinement was performed on X-ray diffraction patterns of run products taking into account microanalysis results (fig. 5). Since no structural data are available for the 10Å phase, a phlogopite structure was considered in which the potassium atomic positions have been replaced by oxonium ions (H_3O^+). The results of background-modelling curve, unit cell and peak-profile parameters refinement in term of phase abundances and lattice parameters are shown in Table 5. Phase abundances were also modelled on a chemical basis via a least squares mass balance calculation and results obtained through the two completely independent methods are in good agreement. Discrepancies might be ascribed to the

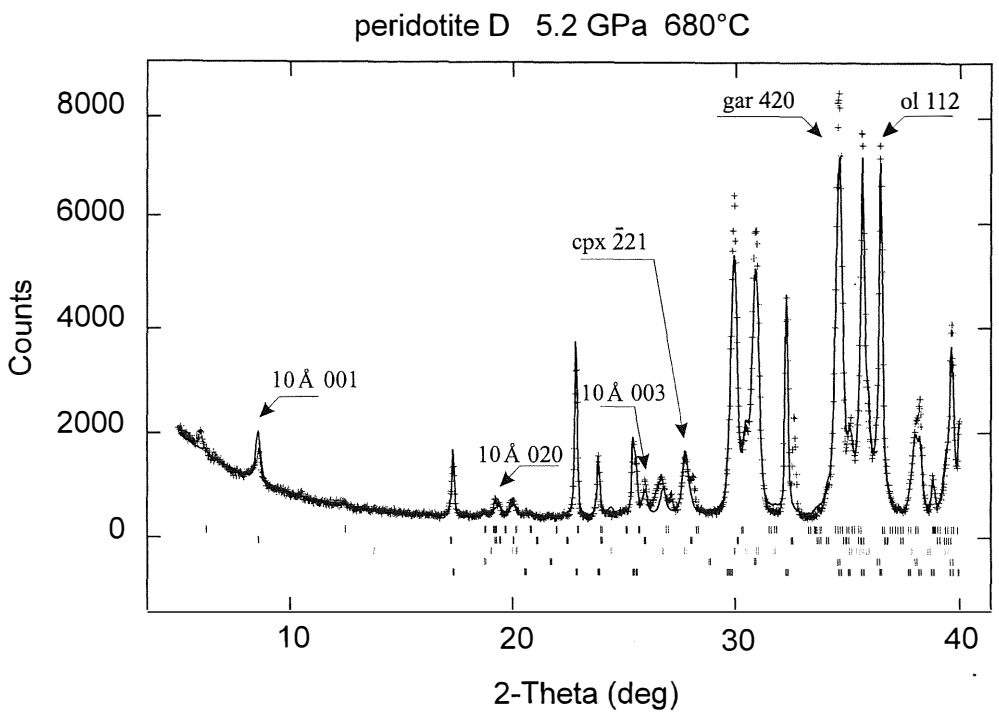

Fig. 5 – X-Ray diffraction profile of run products obtained at 5.2 GPa and 650°C. Crosses represent the observed profile, the continuous line is the calculated profile. Diffractions of phases present are from the bottom to the top: olivine, garnet, diopside, 10Å phase, clinochlore.

presence of seed relics and/or to heterogeneities in mineral compositions, as well as to the approximations assumed for the crystal structure of 10Å phase. The low amount of olivine present is directly related to the high Al and Ca contents in the starting material which maximize the amount of garnet and clinopyroxene. Orthopyroxene and 10Å phase are mutually exclusive and attempts to model a five phase assemblage where both 10Å phase and orthopyroxene are present always indicate the incompatibility of these two phases.

As a consequence, by comparing the two assemblages (Chl3 and Chl2) a reaction responsible for the dehydration of the 10Å phase may be envisaged. The decrease of garnet and the disappearance of orthopyroxene in Chl3 with respect to Chl2 give reason for the reaction:

Al-10Å phase = enstatite + pyrope + H_2O (1),

whose stoichiometric coefficients depend on Al-partitioning between the participating phases. The location of this continuous reaction in P-T space is also related to the dilution of pyrope component with almandine and grossular. Therefore, Ca- and Fe- enrichment of Gel D possibly displaces reaction (1) to lower temperatures compared to depleted lherzolites or harzburgites which are expected to occur in subducted oceanic crust.

It should be noted in fig. 5 that the peak at $2\theta = 5.96$ in X-ray powder diffraction profile of Chl3 can be interpreted either as a relict of chlorite seeds or as newly formed chlorite layers eventually interstratified to the structure of the 10Å phase giving a mixed-layered 10Å phase structure. Such hypothesis is further supported, in analogy to diffraction patterns of mixed-layered chlorites, by the basal peak position of chlorite which is at a greater *d* value than that expected for clinochlore. In such a case the aluminium content, homogeneously

TABLE 5

Results of Rietveld refinement and mass balance.

Phase	**Lattice parameters**		**Phase abundances (Rietveld refinement)**		**Mass balance**	
	Chl2	Chl3	Chl2	Chl3	Chl2	Chl3
olivine	a= 4.7650(3) Å b=10.2319(7) Å c = 5.9957(5) Å V= 292.32(3) Å^3	a= 4.7648(2) Å b=10.2307(4) Å c= 5.9958(3) Å V= 292.28(1) Å^3	26%	30%	33%	35%
clinopyroxene	a= 9.725(2) Å b= 8.899(2) Å c= 5.252(1) Å β= 106.06(1)° V= 436.81(9) Å^3	a= 9.7113(2) Å b= 8.875(1) Å c= 5.2515(6) Å β=106.189(9)° V= 434.69(6) Å^3	28%	33%	34%	32%
garnet	a= 11.5642(5) Å V= 1546.5(2) Å^3	a= 11.5877(4) Å V= 1555.9(1) Å^3	39%	33%	31%	24%
orthopyroxene	a= 18.24(1) Å b= 8.848(6) Å c= 5.243(5) Å V= 846.4(7) Å^3	-	7%	-	1%	-
10Å phase	-	a= 5.340(6) Å b= 9.23(1) Å c=10.454(6) Å β= 100.0(1)° V= 507.5(4) Å^3	-	4%	-	9%

distributed on the scale of microprobe analyses (i.e. μm) could be the result of «averaging» of Al-bearing layers, i.e chlorite layers, and Al-free-10Å phase layers. This possibility cannot be ruled out on a chemical basis. Chemographic projection of fig. 6 shows that all analyses obtained on 10Å phase aggregates of fig. 4 are roughly collinear with chlorites and MSH 10Å phase. TEM investigations are in progress to solve this problem. However it should be noted that the homogeneity on a macroscopic scale and the absence of a complete diffraction pattern of chlorite suggest the occurrence of a single phase and not of an intergrowth of two phases (e.g. MSH 10Å phase + chlorite).

Therefore, whether an aluminous 10Å phase or a mixed-layered 10Å phase is the stable aluminous hydrous phase at the PT conditions investigated, its relevance for ultramafic compositions may be envisaged. In fig. 7 the run products obtained at 5.2 GPa and 680 °C are projected from olivine in the model system CaO-Al_2O_3-SiO_2-H_2O. Also reported are four

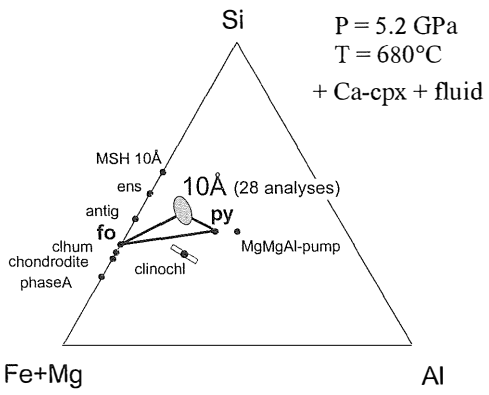

Fig. 6 – Compositional field of aluminous 10Å phase synthesized at 5.2 GPa, 650°C in the system MgO-Al_2O_3-SiO_2.

different bulk compositions corresponding to harzburgite and three lherzolites showing different degrees of Al- Ca- enrichment (compositions A, B, C, D from Mysen and Boettcher, 1975). Lines joining the bulk compositions to the vertex H indicate different degree of hydration. At water undersaturated conditions, e.g. inside the volume, aluminium stabilizes a 10Å phase in association with

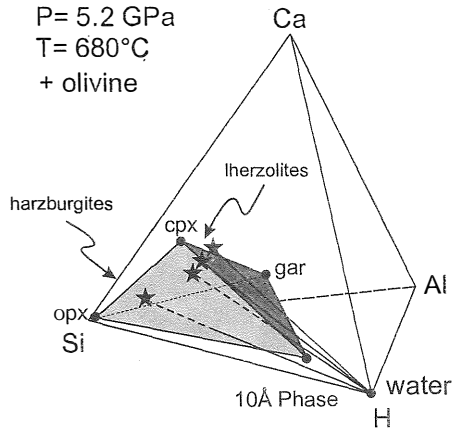

Fig. 7 – Chemography of phases obtained at 5.2 GPa and 650°C in the system CaO-Al_2O_3-SiO_2-H_2O projected from olivine. Four representative anhydrous peridotites (from harzburgite, to lherzolites and pyroxenite, Mysen and Boettcher, 1975) are also plotted.

orthopyroxene, clinopyroxene and garnet both in harzburgites and in lherzolites. At water saturated conditions the 10Å phase coexists in harzburgites with orthopyroxene and forsterite while in lherzolites it coexists with garnet and forsterite. Even though the assemblage 10Å phase + forsterite is incompatible with the join enstatite + H_2O in the simple system MSH, the stable coexistence of all of these phases is possible in Fe- and Al-bearing systems (lherzolites and pyroxenites).

In order to evaluate the role of the 10Å phase in ultramafic slab components at ca. 5 GPa and 680°C, we profit of recent compilations of phase relationships of hydrous peridotites given by Ulmer and Trommsdorff (1999) and by Schmidt and Poli (1998). The comparison of phase relationships for H_2O-bearing ultramafic systems with representative geotherms for subducted slab surfaces obtained by thermomechanical modelling of subduction zones (Kincaid and Sacks, 1997) constrains the (continuous or discontinuous) reactions involving hydrous phases in altered peridotites, the depth to which H_2O is transported in such

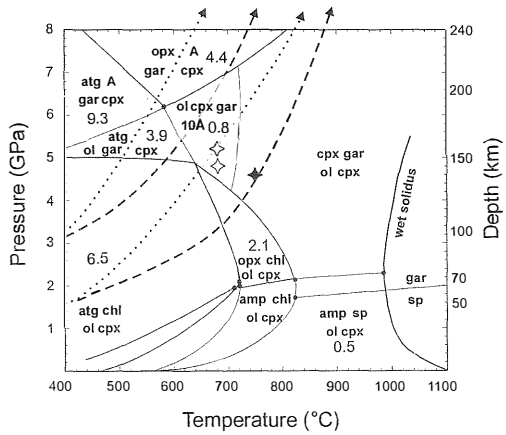

Fig. 8 – P-T diagram compiled from experimental results (modified from Schmidt and Poli, 1998). A wide range of P-T paths typical of subducted slab surfaces are represented by dashed curves, from Kincaid and Sacks (1997), and dotted curves, Davies and Stevenson (1992). Numbers represent the amount of H_2O bounded to hydrous phases in a lherzolitic composition. Filled diamonds: garnet, clinopyroxene, olivine, orthopyroxene; open diamonds: 10Å phase, garnet, clinopyroxene, olivine.

hydrous phases, and the depth range of fluid release to the mantle wedge.

The phase diagram of fig. 8 (modified from Schmidt and Poli, 1998) shows that chlorite and antigorite are the major H_2O reservoirs in a wide temperature range up to ca. 5 GPa, i.e. to ca. 150 km depth. At higher pressures, the transfer of H_2O from antigorite to Dense Hydrous Magnesian Silicates, namely phase A, is possible only for very cold geotherms, as a result of backbending of antigorite breakdown reactions.

If antigorite and chlorite are the only hydrous phases stable in the pressure range from ca. 3 to 6 GPa, their breakdown at temperatures above ca. 600°C implies full dehydration of the assemblage and a dramatic flux of H_2O to the mantle wedge between 120 and 150 km depth. If, on the contrary, as suggested by the preliminary results presented here, a 10Å phase is stable as depicted schematically in the shaded field of fig. 8, on the high pressure side of the chlorite stability field, and on the high temperature side of the antigorite stability field, full dehydration is inhibited and some H_2O might be transferred to phase A at higher pressures. Assuming an average H_2O content in 10Å phase in the order of 9 wt% (Bauer and Sclar, 1981) and phase proportions obtained by mass balance calculations, a total amount of ca. 0.8 wt% H_2O is still stored in a hydrous peridotite outside the chlorite and antigorite stability field but containing the 10Å phase. However, given the estimates of H_2O contents bound in hydrous phases by Schmidt and Poli (1998), 1-3 wt% H_2O are relased when pressure-temperature paths for altered subducted peridotites passes through the 10Å phase field.

Conclusions

Synthesis experiments at 4.6-5.2 GPa pressures and 680-750°C temperatures in the model hydrous peridotites system Na_2O-CaO-FeO-MgO-Al_2O_3-SiO_2-H_2O show that a 10Å phase structure is crucial to unravel the devolatilization history of the subducted oceanic lithosphere. Despite the strict chemographic constraints in simple model systems (MSH) downgrade the occurrence of the 10Å phase to unusual Si-rich compositions, addition of Al and Fe in the reference ultramafic system stabilizes this hydrous phase in a wide range of ultramafic rocks, from harzburgites to lherzolites and pyroxenites. The stability of a 10Å phase beyond the antigorite +/- chlorite field, promotes the transfer of H_2O to phase A and, therefore, to the deepest portion of subducted slabs.

Acknowledgments

Thoughtful and constructive reviews by M. Scambelluri and M.W. Schmidt are gratefully acknowledged. All experimental and analytical work was funded by CNR (CSGAQ) and MURST (Cofin98).

References

Bauer J.F. and Sclar C.B. (1981) — *The «10Å phase» in the system MgO-SiO_2-H_2O.* Am. Mineral., **66**, 576-585.

Boillot G., Girardeau J. and Kornprobst J. (1988) — *Rifting of the Galicia margin: crustal thinning and enplacement of mantle rocks on th seafloor.* Proceedings of the Ocean Drilling Program, Scientific Results, **103**, 741-756.

Davies J.H. and Stevenson D.J. (1992) —*Physical model of source region of subduction zone volcanics.* J. Geophys. Res., **97**, 2037-2070.

Evans B.W. and Trommsdorff V. (1978) — *Petrogenesis of garnet lherzolite, Cima di Gagnone, Lepontine Alps.* Earth Planet. Sci. Lett., **40**, 333-348.

Freuh-Green G. L., Plas A. and Lécuyer CH. (1996) — *Petrologic and stable isotope constraints on hydrothermal alteration and serpentinization of the shallow mantle at Hess Deep (site 895).* In: Mével C., Gillis K.M., Allan J.F. and Meyer P.S. (Eds): Proceedings of the Ocean Drilling Program, Scientific Results, **147**, 255-291.

Hamilton D.L. and Henderson C.M.B. (1968) — *The preparation of silicate composition by gelling method.* Min. Mag., **36**, 832-838.

Khishina N. R. and Wirth R. (1998) — *Water-bearing Fe-Mg silicate inclusions in kimberlitic olivine: high pressure hydrous silicates (DHMS) from mantle?* Terra Nova Abstracts Supplement, **1**, 29.

KINCAID C. and SACKS I.S. (1997) — *Thermal and dynamical evolution of the upper mantle in subduction zones.* J. Geophys. Res., **102**, 12295-12315.

LARSON A.C. and VON DREELE R.B. (1998) — *GSAS General Structure Analysis System.* Report LAUR 86-748. Los Alamos National Laboratory, Los Alamos, New Mexico.

LLOYD E.C. (1971) — Accurate characterization of the high pressure environment. NBS Special Publication No. 326, Washington DC pp 1-3.

MULLER M. R., ROBINSON C.J., MINSHULL T.A., WHITE R.S. and BICKLE M.J. (1997) — *Thin crust beneath ocean drilling program boreholre 735B at the Southwest Indian Ridge.* Earth Planet. Sci. Lett., **148**, 93-107.

MYSEN B.O. and BOETTCHER A.L. (1975) — *Melting of a Hydrous Mantle: I. Phase relations of natural peridotite at high pressures and temperatures with controlled activities of water, carbon dioxide, and hydrogen.* J. Petrol., **16**, 520-548.

MYSEN B.O., ULMER P., KONZETT J. and SCHMIDT M.W. (1998) — The upper mantle near convergent plate boundaries. In Hemley R. J. (ed.): Ultrahigh-pressure mineralogy: physics and chemistry of the Earth's deep interior. Rev. Mineral., **37**, 97-138.

NIIDA K. and GREEN D.H. (1999) — *Stability and chemical composition of pargasite amphibole in MORB pyrolite under upper mantle conditions.* Contrib. Mineral. Petrol., **135**, 18-40.

OBATA M. and MORTEN L. (1987) — *Transformation of spinel lherzolite to garnet lherzolite in ultramafic lenses of the Austridic crystalline complex, northern Italy.* J. Petrol., **28**, 599-623.

PAWLEY A.R. and WOOD B.J. (1995) — *The high-pressure stability of talc and 10Å phase: Potential storage sites for H_2O in subduction zones.* Am. Mineral., **89**, 998-1003.

SCAMBELLURI M., MUENTENER O., HERMANN J., PICCARDO G., TROMMSDORFF V. (1995) — *Subduction of water into the mantle; history of an Alpine peridotite.* Geology, **23**, 459-462.

SCLAR C.B., CARRISON L.C. and SCHARTZ C.M. (1965) — *High-pressure synthesis and stability of a new hydronium-bearing layer silicate in the system Mgo-SiO_2-H_2O.* Transaction of the American Geophysical Union, **46**, 184.

SCHMIDT M.W. and POLI S. (1998) — *What causes the position of the volcanic front? Experimentally based water budget for dehydration slabs and consequences for arc magma generation.* Earth Planet. Sci. Lett., **124**, 105-118.

SUSAKI J. AKAOGI S. and SHIMURA O. (1985) — *Garnet-perovskite transformation in $CaGeO_3$: in-situ X-ray measurements using synchrotron radiation.* Geophys. Res. Lett., **12**, 729-732.

ULMER P. and TROMSDORFF V. (1999) — *Phase relations of hydrous mantle subducting to 300 km.* In: Y-W. Fei, C. Bertka, and B.O. Mysen, Eds. Mantle Petrology: Field observations and high-pressure experimentation, in press. Geochem. Soc.

WALKER D. (1991) — *Lubrication, gasketing, and precision in multianvil experiments.* Am. Mineral., **76**, 1092-1100.

WALTER M.J., THIBAULT Y., WEI K., LUTH R.W. (1995) — *Characterizing experimental pressure and temperature conditions in multianvil apparatus.* Can. J. Phys., **73**, 273-286.

WIRTH R. and KHISHINA N.R. (1998) — *Oh-bearing crystalline inclusions in olivine from kimberlitic peridotite (Udachnaya-East, Yakutiya).* American Geophysical Union Transactions, **79** (45), 882.

YAMAMOTO K. and AKIMOTO S.I. (1977) — *The system MgO-SiO_2-H_2O at high pressures and temperatures-stability field for hydroxyl-chondrodite, Hydroxyl-clinohumite and 10Å phase.* Am. J. Sci., **277**, 288-312.

ZHANG J., LI B., UTSUMI W. and LIEBERMANN R.C. (1996) — *In situ X-ray observations on the coesite-stishovite transition: Reversed phase boundary and kinetics.* Phys. Chem. Min., **23**, 1-10.